02

Chemical pressure, structural instability, and IR-active phonons in a series of rare-earth analogues of francisite $Cu_3RE(SeO_3)_2O_2Cl$

© N.N. Novikova[1], V.A. Yakovlev[1], E.S. Kuznetsova[2], P.S. Berdonosov[2], S.A. Klimin[1]¶

[1] Institute of Spectroscopy, Russian Academy of Sciences, Troitsk, Moscow, Russia
[2] Lomonosov Moscow State University, Chemical Faculty, 119991 Moscow, Russia

¶ e-mail: klimin@isan.troitsk.ru

Received July 22, 2021
Revised July 22, 2021
Accepted August 05, 2021

ATR and transmission spectra of a series of rare-earth francisite-like phases $Cu_3RE(SeO_3)_2O_2Cl$ (RE is a rare earth element, RE = Nd, Sm, Eu, Gd, Dy, Ho, Tm, Yb) were studied. The frequencies of the IR-active phonons of the crystals under study were determined. In the dependences of phonon frequencies on the ionic radius in a series of isostructural compounds, two tendencies are observed: a hardening of frequencies due to an increase in chemical pressure and a softening of the vibration frequencies, in which rare-earth ions are involved, due to an increase in the mass of a specific rare-earth ion. In the $Cu_3Dy(SeO_3)_2O_2Cl$ crystal, an anomalous softening of low-frequency phonons at low temperatures was observed, which was apparently associated with the structural instability of the compound.

Keywords: rare-earth francisite-like phases, optical spectroscopy, IR-active phonons, chemical pressure.

DOI: 10.21883/EOS.2022.01.52986.22-21

Introduction

The phonon spectrum carries important information about the medium. It is genetically related to the crystal structure and therefore is a means of the structure identification and phase transitions investigation. Phonons are involved in varying degrees in the interactions of various subsystems: lattice, charge, and magnetic. Such interactions can lead both to the formation of bound modes and to unusual behavior of phonons. In the works of Professor Marina Popova, whose anniversary this paper is dedicated to, important results were obtained relating the study of multifunctional materials using the spectroscopy of vibrational states in the field of lattice dynamics [1–7], structural [8–10] and magnetostructural transitions [6,11–13], spin-phonon [4,9,14–16], electron-phonon [17–20] and interionic (Davydov) [21] interactions, magneto-dielectric [18] and isotopic [22] effects, bound electron-phonon [14,19] and magnon-phonon [3] modes. In this paper, based on the experience gained thanks to the joint work with the hero of the day, we are conducting the first study of the spectrum of infrared active phonons of new rare-earth compounds of the francisite family.

A family of rare-earth analogues of the francisite mineral with the general chemical formula $Cu_3RE(SeO_3)_2O_2Cl$ (RE is rare-earth element, REE) was first synthesized relatively recently [23,24] and attracted the attention of the scientific community due to its interesting magnetic [25–31] and multiferroic [32] properties. The ancestor of the family is a natural mineral of the same name (francisite), oxoselenite-copper(II) bismuth chloride $Cu_3Bi(SeO_3)_2O_2Cl$ [33], discovered for the first time in 1987 at the Iron Monarch mine (Australia) by Glyn Francis, whose name was included in the name of the mineral. Such a combination of elements has never been seen before in mineralogy [34]. Further, chemists were able to synthesize in the laboratory both the crystal itself, corresponding to the composition of francisite, and numerous derivatives of it, replacing chlorine with other halogens (bromine and iodine) [34], selenium with tellurium [35] and bismuth with REE. $Cu_3Er(SeO_3)_2O_2Cl$ [36] became the first synthetic francisite with REE, and almost a complete series of them was synthesized at the Lomonosov Moscow State University [23,24]. As a result, a large set of isostructural compounds is a model range for studying the systematic features of various properties, including chemical, structural, magnetic, and vibrational ones.

The crystal structure of the francisite mineral was determined in 1990 [33] and later confirmed in a number of papers [37–39]. It crystallizes in rhombic system, space group $Pmmn$. All currently known francisite-like phases with REE also belong to this space group at room temperature. For them, an almost monotonous increasing of three parameters of the crystal lattice a, b and c, as well as the volume of the unit cell V is observed with increasing of REE ionic radius [23]. Figure 1 shows fragments of the crystallographic structure of francisite. The main features of the crystal lattice are: *1* — magnetic planes of the copper sublattice, *2* — hexagonal channels containing halogen atoms, *3* — molecular selenite groups $(SeO_3)^{2-}$. The magnetic planes are arranged in such a way that copper ions form the so-called kagome lattice (see projection ab, Fig. 1), which is not 2D, which is clearly seen in the projection ac, Fig. 1. Frustrations characteristic

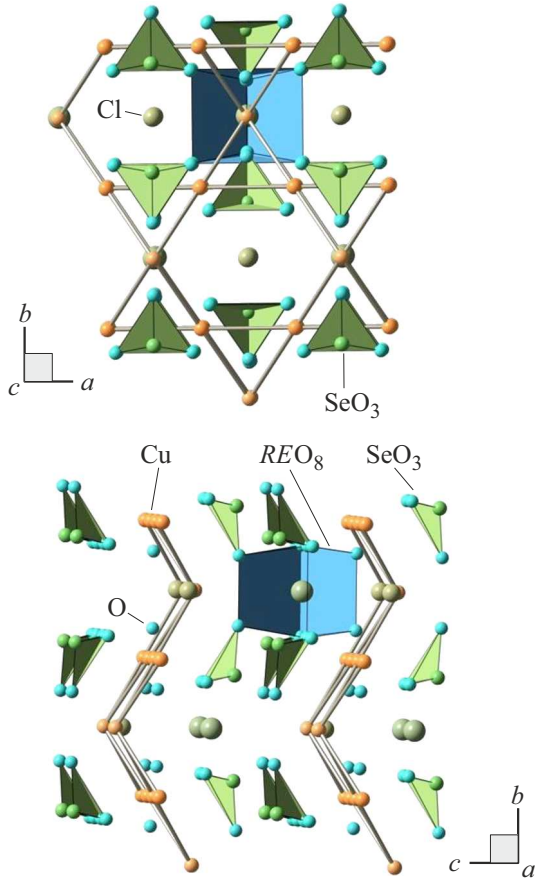

Figure 1. Fragment of crystalline structures of francisite-like phases $Cu_3RE(SeO_3)_2O_2Cl$, view along crystallographic axis c (upper panel) and axis a (lower panel). The triangular distorted pyramids SeO_3 and one polyhedron REO_8 are shown. The nearest copper atoms are bonded to emphasize the presence of 2D planes and the nature of the magnetic lattice in plane. Chlorine atoms are located inside hexagonal channels directed along the axis c.

for the kagome lattice, due to the strong competition of ferromagnetic and antiferromagnetic interactions in copper planes, do not manifest themselves explicitly, however, they must be taken into account, and their role in the magnetism of francisite and its analogs is widely discussed in the literature [40–43].

Hexagonal channels are clearly visible on the projection ab (Fig. 1). Inside the channels chlorine atoms are located, as well as unshared electron pairs of selenium, which require a certain amount of space. The channels have different sizes in compounds with various triple-charged ions, while this size increasing leads to a higher mobility of halogen atoms, which, in particular, according to paper [43], is the cause of the structural phase transition observed in $Cu_3Bi(SeO_3)_2O_2Cl$ with temperature decreasing ($T_C = 115$ K). In this sense, it seems interesting to compare the phonon spectrum in a series of compounds with different channel sizes, since the phase transition in $Cu_3Bi(SeO_3)_2O_2Cl$ is accompanied by a change in the spectrum of both IR and RSS active vibrations.

Molecular selenite groups $(SeO_3)^{2-}$ are complexes isolated from each other with the strongest interatomic bonds. As a rule, such complexes, for example $(BO_3)^{2-}$ [9,14], $(PO_4)^{3-}$ [44], $(MoO_4)^{2-}$ [10], as well as $(SeO_3)^{2-}$ placed in a crystalline environment retain vibration frequencies close to the frequencies of the free complex, which greatly simplifies the analysis of the phonon spectrum. The vibration properties of the selenite group $(SeO_3)^{2-}$ were previously studied for a number of compounds [45–48]. To analyze the contribution of the selenite group to the phonon spectrum of francisite-like phases it is necessary to carry out a correlation analysis for the normal vibrations of the group $(SeO_3)^{2-}$ and comparison with experimental data.

The phonon spectrum of francisite-like phases has been studied in detail only for bismuth-containing compounds, which can be grown in the form of single crystals, in contrast to their analogs with REE, which can only be synthesized in a polycrystalline form. In the paper [48] the infrared reflection spectra in polarized light were studied, and the spectroscopic parameters of IR-active phonons of symmetry B_{1u}, B_{2u} and B_{3u} were determined for $Cu_3Bi(SeO_3)_2O_2Cl$ crystal. In the paper [32] the Raman spectroscopy (RSS) spectra were studied and information was given on the frequencies of RSS-active phonons of symmetry A_g and B_{1g}. Information on the phonon spectrum of francisite-like phases, as far as we know, is not available in the literature.

In this paper, for the first time, a systematic study of infrared (IR) spectra in the phonon region of a number of synthetic analogs of francisite containing REE $Cu_3RE(SeO_3)_2O_2Cl$ (RE = Nd, Sm, Eu, Gd, Dy, Ho, Tm, Yb) was performed to determine the parameters of IR-active phonons and search for regularities in the behavior of vibration modes in a series of isostructural compounds with different lattice parameters and REE ions of different masses. For $Cu_3Dy(SeO_3)_2O_2Cl$ the temperature variations of the phonon parameters were studied in order to search for low-temperature anomalies.

Experiment methods

The studied compounds were synthesized using lanthanide oxides Ln_2O_3 (Ln = Nd, Sm, Eu, Gd, Dy, Ho, Tm, Yb) (Giredmet, Russia, 99.99% minimum), copper(II) oxide CuO (purity 9−2), anhydrous copper(II) chloride $CuCl_2$ (Sigma-Aldrich $\geq$ 99.995%) and selenium(IV) oxide SeO_2, previously obtained from selenious acid H_2SeO_3 (chemically pure grade) by dehydration in vacuum at a temperature of 70−90°C and sublimated in a stream of dried air with NO_2.

Samples with SeO_2 were taken in a dry box purged with argon. The precursors listed above were used to prepare stoichiometric mixtures in accordance with the reaction

equation:

$$5CuO + CuCl_2 + Ln_2O_3 + 4SeO_2 = 2Cu_3Ln(SeO_3)_2O_2Cl. \quad (1)$$

Precursors were weighed on a Sartorius Gemp^{lus} balance with an error of 0.0002 g with a total weight of sample for each composition 1 g maximum. The mixtures of initial substances obtained for each composition were thoroughly ground in an agate pounder and placed in quartz ampoules, which were then soldered under vacuum $\sim 10^{-2}$ mm Hg. After that, each of the mixtures was annealed in a furnace in the following mode: heating to 300°C for 12 h, holding at a constant temperature for 24 h, heating to 575°C for 6 h, keeping at this temperature for 72 h.

As a result, powdered compounds of green color with uniform color were obtained. X-ray phase analysis performed using STOE Stadi-P diffractometer (source Cu$K_{\alpha 1}$) confirmed the single-phase nature of the obtained compounds. The X-ray patterns of all products were similar to each other and were fully indexed in the space group *Pmmn*. The unit cell parameters fully correspond to the data of the paper [23].

To study the IR spectra of total internal reflection, an ATR accessory with a diamond prism was used, the angle of incidence was 45°. The measurements were carried out on a BRUKER IFS66 v/s Fourier spectrometer in a wide spectral range from 50 to 2000 cm^{-1} in two steps: in the far IR range from 50 to 550 cm^{-1} and in the mid IR range from 400 to 5000 cm^{-1}, the spectral resolution was 4 cm^{-1}. In both cases, the radiation source was a globar, which is a silicon carbide (SiC) rod heated to high temperatures. In the long-wavelength spectral region, a lavsan beam splitter with a coating of germanium and a pyroelectric receiver based on DLATGS (deuterated triglycine sulfate with an admixture of L-α-alanine) were used; KBr beam splitter and pyroelectric receiver based on DTGS (deuterated triglycine sulfate $(NH_2CH_2OOH)_3 \cdot H_2SO_4$) were used in short-wavelength region. To reduce noise in the low-frequency region, the spectra were additionally measured using a helium bolometer, at that the measurements were carried out on BRUKER IFS125HR Fourier spectrometer.

The temperature-dependent diffuse transmission spectra of the dysprosium analogue of the francisite mineral $Cu_3Dy(SeO_3)_2O_2Cl$ were measured on BRUKER IFS125HR Fourier spectrometer. The polycrystalline sample was crushed in an agate pounder, after which a finely dispersed suspension of the compound under study in alcohol was prepared. The suspension was deposited on a diamond plate and, after drying, a thin uniform film formed on the diamond surface. After that, the diamond with the formed film was tightly pressed using an indium spacer to the cold pipe of CRYOMECH PT403 optical helium cryostat with polyethylene optical windows.

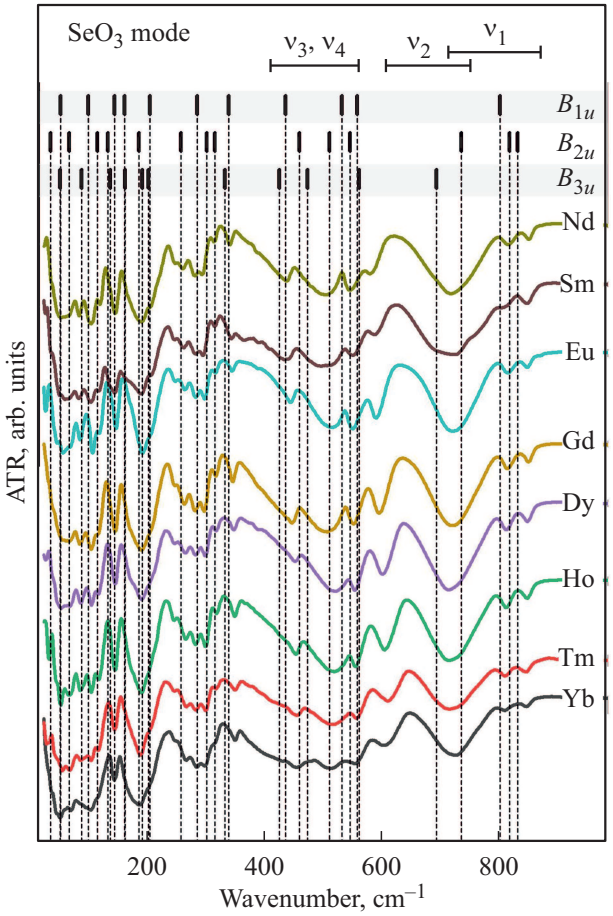

Figure 2. Experimental spectra of ATR for rare-earth analogues of francisite $Cu_3RE(SeO_3)_2O_2Cl$ (RE = Nd, Sm, Eu, Gd, Dy, Ho, Tm, Yb) in wide spectral region measured at room temperature. The spectra are arbitrarily shifted along the ordinate axis for clarity. Dashes with falling vertical dashed lines correspond to TO frequencies for $Cu_3Bi(SeO_3)_2O_2Cl$ crystal [48]. Above, the frequency intervals for internal vibrations of molecular complexes $(SeO_3)^{2-}$ are shown.

Study results and discussion

The spectra of attenuated total reflection (ATR) of francisite-like phases $Cu_3RE(SeO_3)_2O_2Cl$ (RE = Nd, Sm, Eu, Gd, Dy, Ho, Tm, Yb) in a wide spectral range are shown in Fig. 2. The spectra for the eight compounds presented are similar, this was expected for a series of isostructural compounds. This fact is also an indirect confirmation of the fact that, indeed, all compounds have the same crystallographic structure.

Factor-group analysis gives the following formula for the optical vibrational modes of francisites with structure *Pmmn* [32,48]:

$$\Gamma_{opt} = 14B_{1u}(E \parallel z) + 14B_{2u}(E \parallel y) + 11B_{3u}(E \parallel x) + 12A_g(xx, yy, zz) + 6B_{1g}(xy, yx) + 9B_{2g}(xz, zx) + 12B_{3g}(xy, yx) + 9A_{1u}. \quad (2)$$

The activity of vibrational modes is indicated in parentheses: in the direction of the electric field **E** of the light wave for IR-active phonons and in the direction of the electric field of the incident and analyzed radiation for RSS-active modes. Symmetry modes A_{1u} are optically inactive.

According to formula (2), total number of IR-active modes to be observed in the crystals of the studied phases of the structure *Pmmn* should be 39. However, as it follows from the data of paper [48], the IR modes are strongly overlapped in $Cu_3Bi(SeO_3)_2O_2Cl$ crystal: some vibration frequencies of different symmetry have very close values. Moreover, the authors of this paper, having registered in two polarizations exactly as many IR-active modes quantitatively as expected from the factor-group analysis, could detect only 11 out of 14 IR-active modes of symmetry B_{1u} in the third polarization, as likely also due to the closeness of the frequencies of some modes. Besides, we emphasize that the data in this paper were obtained at helium temperature (7 K), when the damping of phonon modes is minimal. At room temperature, the overlap increases due to phonons widening. Indeed, a comparison of the transmission spectra of $Cu_3Dy(SeO_3)_2O_2Cl$ crystal measured at room (300 K) and low (15 K) temperatures clearly shows that due to thermal widening and overlapping many lines (marked by arrows in Fig. 3, *a*) become unresolvable at high temperatures. With such a large number of phonons and the impossibility of measuring polarized spectra on polycrystalline samples, it can be assumed that in rare-earth analogues of francisite at room temperature the number of recorded IR modes will be significantly less than the number of modes expected from the theoretical group analysis.

In the ATR spectra measured at room temperature depending on the compound we were able to detect up to 25 peaks, including „branches“ on the wings of strong absorption lines, the frequencies of which are summarized in a Table, which, for comparison, includes data on IR-active phonons for $Cu_3Bi(SeO_3)_2O_2Cl$ from paper [48]. For clarity, Fig. 2 shows a comparison with the data for $Cu_3Bi(SeO_3)_2O_2Cl$ single crystal available in the literature. A good agreement between the obtained data and the literature data is observed, especially if we take into account the frequency shifts caused both by the difference in the crystal lattice parameters and by the weight of the three-charged REE ion.

Note also the well-known fact that the minima in ATR spectra are near the TO-frequencies, but do not coincide with them. To demonstrate this fact we simulated the transmission and ATR spectra using the optical parameters obtained in the paper [48]. The permittivity is determined by the dispersion relation in terms of the sum of contributions N of independent damped oscillators:

$$\varepsilon(\omega) = \varepsilon_\infty + \sum_{j=0}^{N} \frac{S_j \omega_j^2}{\omega_j^2 - \omega^2 + i\gamma_j \omega}, \qquad (3)$$

where ε_∞ is the permittivity at high frequencies, ω_j, S_j and γ_j are the frequency, oscillator strength, and half-width for j-th phonon. The ATR spectra and transmission spectra were calculated using the SCOUT program [49]. Figure 3, *b* compares the calculated ATR and transmission spectra for phonons of symmetry B_{1u} in a limited spectral region. It can be seen that, for low-intensity lines, the position of the minima of the transmission peaks practically coincides with the TO frequencies. For more intensive lines, insignificant shifts are observed in the ATR spectrum.

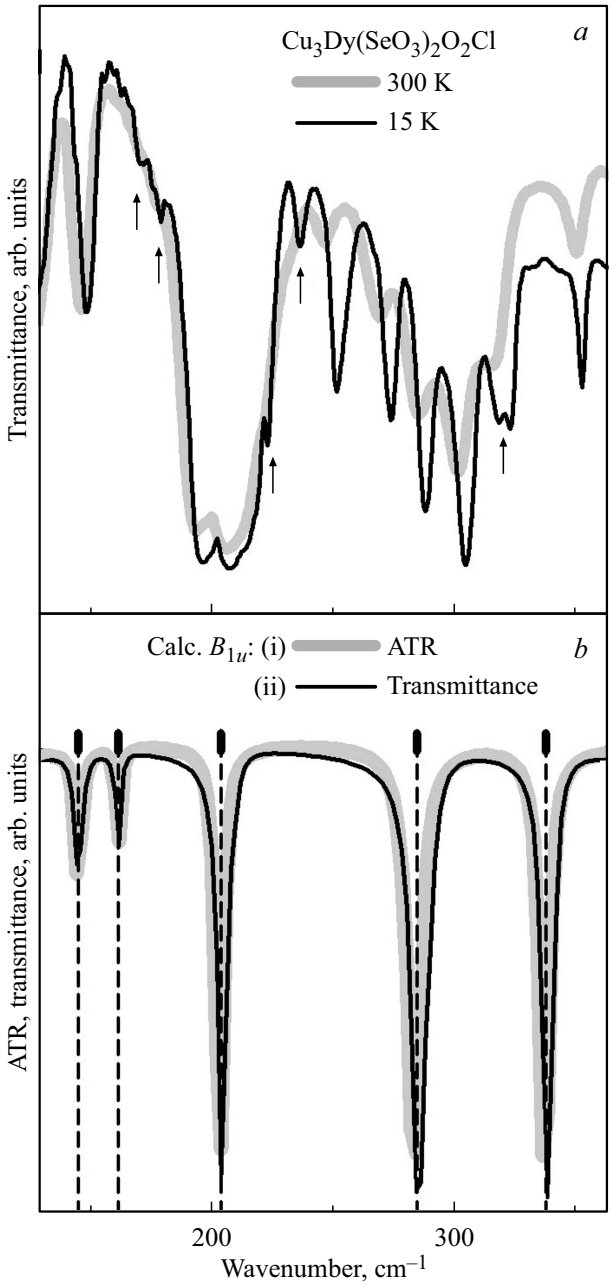

Figure 3. (*a*) Diffuse transmission spectra of polycrystalline $Cu_3Dy(SeO_3)_2O_2Cl$ at room and low (15 K) temperatures. (b) Calculated ATR (thick gray line) and transmission (thin black line) spectra of the $Cu_3Bi(SeO_3)_2O_2Cl$ crystal.

Note that the spectra in Fig. 3 show several groups of lines separated by small intervals. The presence of line groups

Frequencies of IR-active phonons (in cm^{-1}) of phases with structure of francisite $Cu_3RE(SeO_3)_2O_2Cl$ and their correlation with TO-phonons in $Cu_3Bi(SeO_3)_2O_2Cl$ [48]

This paper									[48]
Yb	Tm	Ho	Dy	Gd	Eu	Sm	Nd	Comment	Bi
	32	32.6				31.1		Branch	36.3 (B_{2u})
48.7	45.5	45.1	48.4	40.7	42.2	42.7	41.4		52.8 (B_{3u})
–	56.8	54.1	–		56.5	56.7	56.1		53.2 (B_{1u})
70.4	69.5	68.4	69.1	69.2	69.5	69.2	69.1		68.3 (B_{2u})
89.3	86.9	85.6	85.7	84.7	85.5	84.3	84.4		89 (B_{3u})
104.5	104.9	105	105.3	104.8	106.8	104.8	104.5		99.8 (B_{1u})
116.6	116.2	116.1	116.7	117.2	118.7	118.6	120.1	Branch	115.2 (B_{2u})
143.7	144	144.1	144.9	145.3	145.9	145.1	145.2		133.5 (B_{2u})+ 137.6 (B_{3u})+144.8 (B_{1u})
176.4	175.5	172.3	173.4	170.9	170.6	167.9	169	Branch	161.9 (B_{3u})+161.5 (B_{1u})
187.1	187	188	188.2	189	190	190	190.5		185.8 (B_{2u})+191.6 (B_{3u})
201.6	202.6	202	202	207	205.7	204.9	204	Branch	202.1 (B_{3u})+204 (B_{1u})
245	244.8	244.7	245.1	245.8	246.5	245.4	246.1		256.9 (B_{2u})
266	265	263.2	263	261.8	262.9	260.5	260.1		–″–
282	281.7	281	280.5	280.5	280.9	280.2	279.7		284.4 (B_{1u})
298.1	297.9	297.5	296.5	295.3	296	292.9	291.5	Branch	300.3 (B_{2u})
316.6	316.5	316.3	316.2	315.9	314.6	314.3	312.9		313.9 (B_{2u})
348.5	348.1	346.9	345.9	344	343	341.1	339.2	Branch	331.1 (B_{3u})+337.6 (B_{1u})
426.4	428.4	426.8	425.9	423.6	421.2	424	418.3		422.9 (B_{2u})
454	451.8	448.8	447.1	444.3	440.1	438	433.4		456.3 (B_{2u})+433.5 (B_{1u})
511	512	513	514	507	508	502	500	Wide	470.2 (B_{3u})+507 (B_{2u})
553	553	550.8	549.9	546.9	544.9	545.8	538.7		528.4 (B_{1u})
604	605.4	600.1	596.6	591.2	586.4	584.5	576.9		542.3 (B_{2u})+ 557.3 (B_{3u})+554.4 (B_{1u})
717	712	714	712	716	715.5	718.6	717		688.2 (B_{3u})+730 (B_{2u})
803.9	804.2	805.3	806.6	807.4	808	808	809		811.3 (B_{2u})+794.9 (B_{1u})
840	839.8	840.8	841.3	842.5	842.4	842.3	843.7		825 (B_{2u})

is associated with the possibility of phonons separation into types: into internal vibrations of the molecular group $(SeO_3)^{2-}$ and external with respect to it.

The free complex $(SeO_3)^{2-}$ has the symmetry C_{3v} and has 4 normal vibrations: nondegenerative ν_1 and ν_2 of symmetry A_1 and degenerative ν_3 and $\nu_4(E)$ [50]. We follow this system of notation, although there are discrepancies in the literature. Oscillation ν_1 is often called symmetric (ν_s), ν_2 — asymmetric (ν_{as}), and ν_3 and ν_4 — valence (δ — bending). The frequency of each of the normal vibrations changes slightly when the molecular group is in a particular matrix. Based on the papers [45–47], in which the vibration frequencies of the molecular group $(SeO_3)^{2-}$ in different crystals were studied, we determined the approximate frequency range for each of the vibrations shown on top in Fig. 2. The internal vibrations of the group $(SeO_3)^{2-}$ occupy the highest frequency interval in the phonon spectrum of francisites, while the vibrations ν_1 and ν_2 have the highest frequencies.

To determine the number of modes corresponding to internal vibrations of the selenite complex $(SeO_3)^{2-}$, we performed a correlation analysis in each of the crystal representations. Figure 4 shows a part of this analysis related to internal vibrations $(SeO_3)^{2-}$. The unit cell of

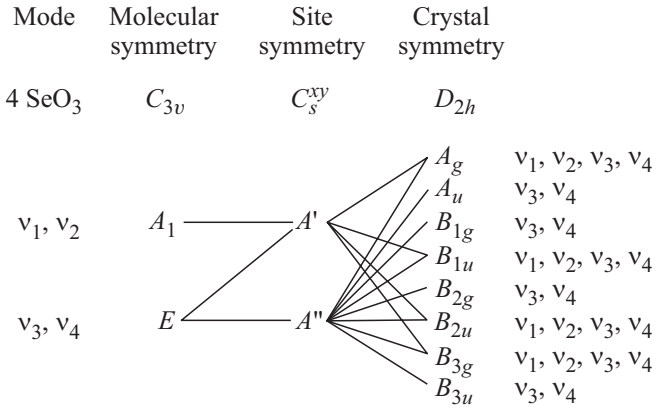

Figure 4. Correlations of internal normal vibrations of group $(SeO_3)^{2-}$ in crystals of tetrahedral symmetry D_{2h}.

francisite crystals of structure *Pmmn* contains 2 formula units and, accordingly, 4 molecular groups SeO_3. In crystal the symmetry of a free molecule C_{3v} decreases to C_s. This distortion is small: if in undistorted molecule three distances Se-O are similar, then in crystal they slightly differ: one distance (calculated for the structure $Cu_3Bi(SeO_3)_2O_2Cl$ [34])

is 1.73 Å, while the other two are equal (for symmetry C_s) and are 1.69 Å. As follows from the correlation scheme, IR-active phonons (2) include two modes for the highest frequency vibrations ν_1 and ν_2, which is in good agreement with the spectra obtained in this paper. Indeed, in the spectral region of frequency ν_1, two absorption bands are observed in the spectra of all eight compounds, while only one band is observed for the vibration ν_2, which, apparently, is a common outline for two overlapping bands. Absorption bands for totally symmetric vibrations ν_1 of various molecular groups are low-intensive (see examples in [14,44]) due to the fact that in free molecule the totally symmetric vibrations do not create a dipole moment, which is necessary for electric dipole interaction with a light wave. A small dipole moment of normal vibrations, correlating with the vibration ν_1, appears when the molecule is in crystal, and its symmetry is lowered.

Figure 5 shows the ATR spectra (in narrow spectral region) of the francisite-like phases studied in this paper. The spectra in the Figure are arranged in such a way that the tabular number of the REE ion included in the compound grows smoothly, when the spectra in Fig. 5 are reviewed from top to bottom. The value of the ionic radius was taken from Shannon Tables [51,52], data for eightfold coordination, which occurs in the structure of francisite analogs containing REE ions.

The absorption peaks in Fig. 5 also smoothly shift from compound to compound, and the nature of these shifts is different. For example, phonon modes near 350, 450 and 500 cm^{-1} shift to the high-frequency side with ionic radius decreasing, while modes near 140 and 170 cm^{-1} shift to the low-frequency region.

These shifts can be explained if consider, firstly, that the unit cell parameters also change smoothly depending on the ionic radius of the rare-earth ion and, secondly, that the mass of the REE ion in the series of compounds under study changes by $\sim 20\%$.

The size decreasing of the unit cell with the ionic radius decreasing of REE can be considered as a phenomenon of „chemical compression“. It is expected that chemical bonds „on average“ will become more rigid when the cell is compressed, which should lead to increased („stiffening“) of vibrational frequencies, which is easy qualitatively understood for a system of two weights connected by a spring, according to the following well-known relation:

$$\nu = \sqrt{\frac{k}{m}}, \qquad (4)$$

where ν is system oscillation frequency, k is spring stiffness, m is reduced mass. According to equation (4), the weighting of atom participating in the given vibration should lead to the vibration frequency decreasing. Thus, the vibrational modes, in which REE ions participate, should also be compound dependent. Since REE is the heaviest of the chemical elements of the compound, normal vibrations, in which rare earth participates, will also have low frequencies.

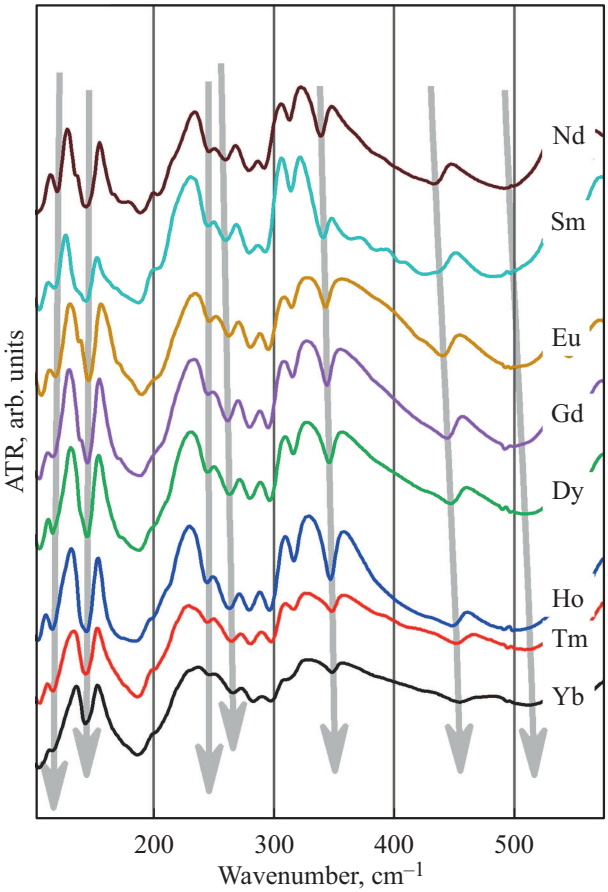

Figure 5. Experimental spectra of ATR for francisite-like phases $Cu_3RE(SeO_3)_2O_2Cl$ (RE = Nd, Sm, Eu, Gd, Dy, Ho, Tm, Yb) in low-frequency spectral region at room temperature. The spectra are arbitrarily shifted along the ordinate axis for clarity. The arrows show the systematic shift of the spectral lines depending on the ionic radius of the rare-earth ion.

Note that in the series of rare-earth ions relevant to this study, upon moving from Yb to Nd the ionic radius, as well as the cell parameters, increases, while the ion mass decreases. Thus, in the considered sequence it is expected that the frequency will decrease due to the effect of chemical compression and increase due to the effect of the ion mass.

Figure 6 shows the dependences on the ionic radius for normalized lattice parameters and for normalized frequencies (energies) of some normal vibrations from the frequency range above 300 cm^{-1}. The values shown on the graph were taken as the ratio of the frequency or lattice parameter in a given compound to the corresponding values for ytterbium francisite. A slight nonlinearity of the lattice parameters b and c is observed, which has some manifestation in the frequency dependences. On the whole, the frequencies depend almost linearly on the ionic radius, which fits into the model of chemical compression: the smaller the REE ionic radius is, the smaller the lattice parameters are, the denser the packing is, the stronger the bonds are, and, accordingly, the higher vibration frequencies are.

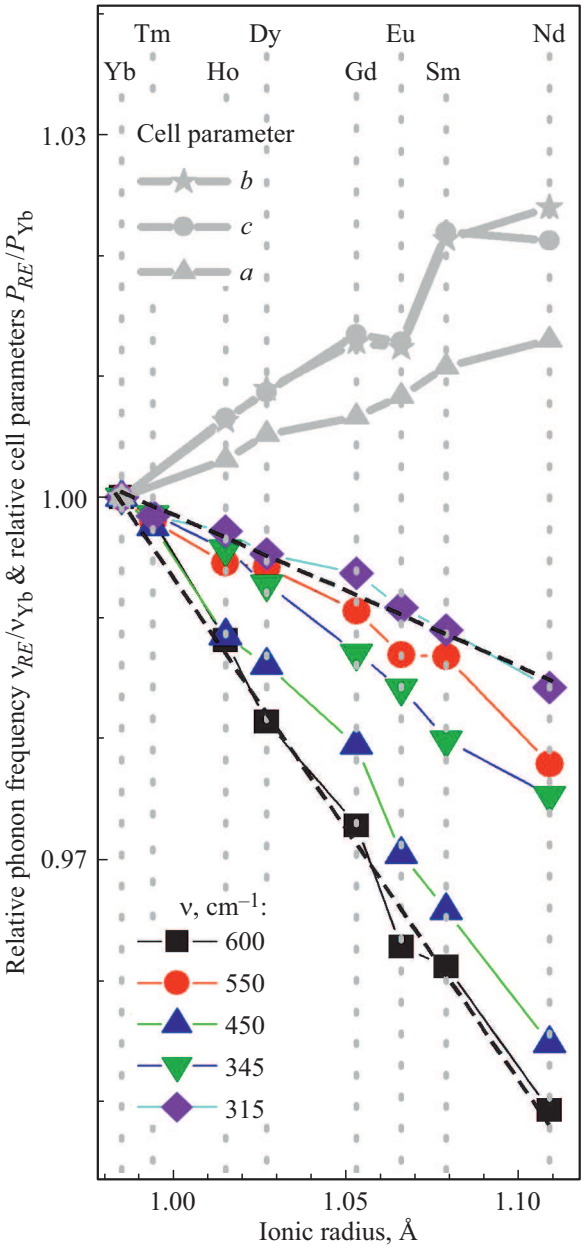

Figure 6. Normalized parameters of lattice (gray symbols) and frequencies (color symbols) of some vibrational modes of francisite-like phases $Cu_3RE(SeO_3)_2O_2Cl$ depending on the ionic radius of the rare-earth ion.

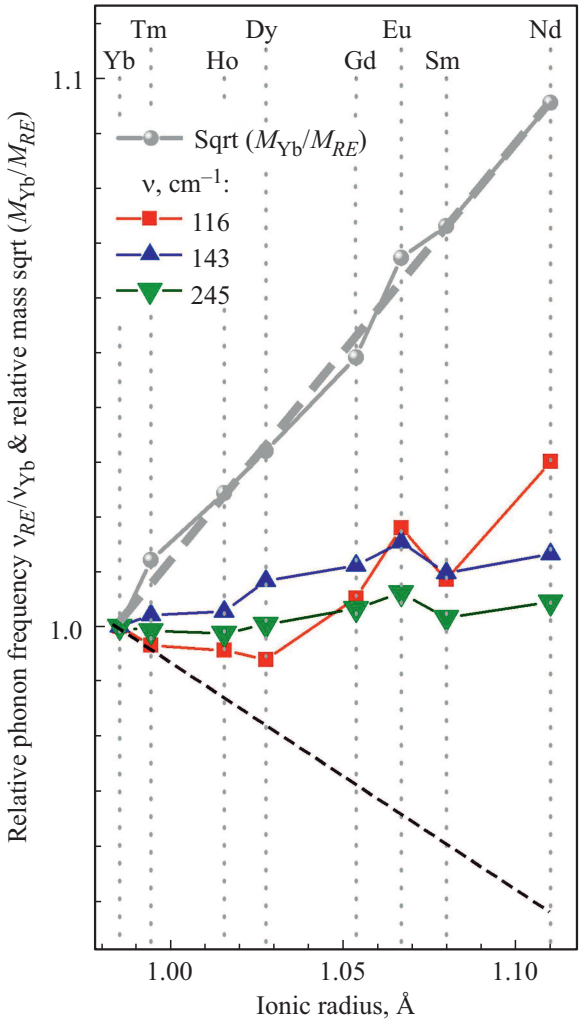

Figure 7. Normalized frequencies of some low-frequency vibrational modes (colored triangles and squares) of francisite-like phases $Cu_3RE(SeO_3)_2O_2Cl$ and the square root of the inverse mass of the rare-earth ion (gray balls and lines) depending on the ionic radius of the rare-earth ion. For comparison, the black dashed line indicates the behavior of the 600 cm^{-1} mode.

Figure 7 shows the normalized frequencies for some low-frequency normal vibrations of the francisite-like phases $Cu_3RE(SeO_3)_2O_2Cl$. These dependences of frequencies on the ionic radius have a completely different nature as compared to the dependences for modes shown in Fig. 6. In general, the frequency of each of the presented modes increases with the ionic radius increasing. We suppose that these modes are associated with vibrations in which the rare-earth ion participates. In addition to frequencies, Fig. 7 shows the dependence of the normalized square root on the reciprocal mass of REE ion ($\sqrt{M_{Yb}/M_{RE}}$). The frequencies of vibrational modes involving the rare-earth ion are affected by both the „mass“factor, and the chemical compression factor; as result upon ionic radius increasing the vibration frequency increases in lesser degree then it can if only mass of ion participating in vibration is considered. Thus, the analysis of the frequency behavior of phonons depending on the ionic radius allows identification of the vibrational modes that are genetically related to the motion of the rare-earth ion.

We also studied the diffuse transmission spectra of $Cu_3Dy(SeO_3)_2O_2Cl$ crystal upon the sample cooling. Figure 8 shows the transmission spectra at three different temperatures: 300, 80, and 7 K. We chose two phonons exhibiting temperature behavior of a different nature. The phonon with frequency near 350 cm^{-1} demonstrates normal behavior. First, the phonon frequency increases with

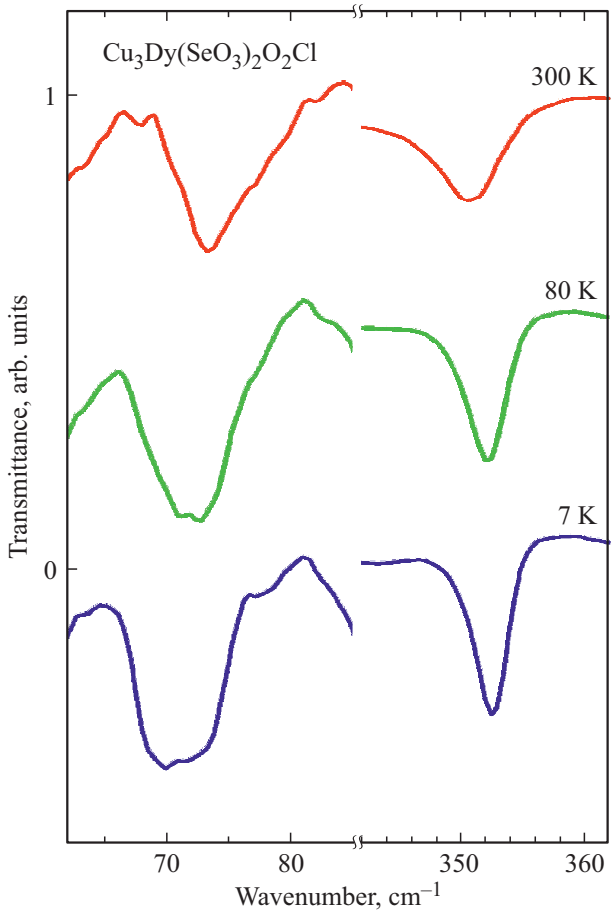

Figure 8. Diffuse transmission spectra of polycrystalline $Cu_3Dy(SeO_3)_2O_2Cl$ at three different temperatures. Two isolated phonons are shown in different regions of the spectrum.

temperature decreasing due to the effect of chemical compression mentioned above. When the crystal is cooled, its size decreases, the interionic bonds become more rigid, which leads to the vibrational frequencies increasing. Secondly, the half-width of this phonon decreases with temperature decreasing. This behavior is normal, since the number of decay processes of this phonon state decreases upon cooling. In particular, due to the population decreasing of vibrational states at low temperatures, only relaxation decay processes remain. Note that almost all phonons in the measured frequency range with frequencies above $100\,cm^{-1}$ behave in a similar way: as the temperature decreases, their frequencies increase, while their half-widths decrease.

Phonons with frequencies below $100\,cm^{-1}$ behave differently depending on the temperature. Firstly, their frequencies decrease with temperature decreasing, and secondly, their half-widths response weakly to temperature changes, and for some phonons even half-width increasing is observed upon cooling. The example of such low-frequency phonon near $70\,cm^{-1}$ is shown in Fig. 8.

This behavior is anomalous. The phonon softening, accompanied by widening, can be regarded as the development of structural instability. In particular, in the paper [14], when studying the structural phase transition in ferroborates, it was found from the results of studies by the IR reflection method that the phonon half-width increases long before the phase transition, being a precursor of structural changes. Recall that the ancestor of the family, i.e. francisite $Cu_3Bi(SeO_3)_2O_2Cl$, experiences the structural phase transition associated with the mobility of halogen atoms, in this case chlorine, inside hexagonal spatial channels. We believe that in the case of $Cu_3Dy(SeO_3)_2O_2Cl$ the structural transition is virtual, impracticable at positive temperatures, and the behavior of low-frequency phonons is an indication of the instability development in the positions of chlorine atoms. The alternative explanation for the anomalous behavior of low-frequency phonons could be the interaction of the lattice and magnetic degrees of freedom in $Cu_3Dy(SeO_3)_2O_2Cl$ crystal. Francisites are low-dimensional magnetics, for which the presence of magnetic correlations is possible at temperatures much higher than the Neel temperature. Moreover, in the paper [40] there are indications of the possible existence of the Thouless-Kosterlitz transition in the family of compounds with the francisite structure, which may result in the formation of correlated magnetic phase with specific vortex excitations. As a result, the interaction of low-frequency phonons with magnetic correlations in the paramagnetic phase, as well as with magnons in the antiferromagnetic phase, can also lead to anomalous behavior of phonons.

Conclusion

The ATR spectra of series of analogs of francisite $Cu_3RE(SeO_3)_2O_2Cl$ (RE — rare-earth element, RE = Nd, Sm, Eu, Gd, Dy, Ho, Tm, Yb) were systematically studied. The obtained dependences of the behavior of phonon frequencies on the ionic radius fit into the model of chemical compression, in which the unit cell parameters decreasing in series of isostructural compounds leads to stiffening of phonons. Phonons, corresponding to vibrations in which REE ions participate, are revealed. For these phonons their softening is observed due to the fact that the influence of the REE ion mass on the frequency prevails over the effect of chemical compression. For the dysprosium compound $Cu_3Dy(SeO_3)_2O_2Cl$ the anomalous softening of low-frequency phonons was found, presumably related to structural instability in the positions of chlorine atoms.

Funding

The work of N.N.N., V.A.Ya. and S.A.K. (spectroscopic studies) was carried out at ISAS and supported by the Russian Foundation for Basic Research under the grant № 19-02-00251, the work of E.S.K. (synthesis of compounds) was carried out at Lomonosov Moscow State University and supported by the Russian Foundation for Basic Research under the grant № 19-33-60093 „Perspektiva“.

Conflict of interest

The authors declare that they have no conflict of interest.

References

[1] N.N. Kuzmin, S.A. Klimin, B.N. Mavrin, K.N. Boldyrev, V.A. Chernyshev, B.V. Mill, M.N. Popova. J. Phys. Chem. Solids, **138**, 109266 (2018). DOI: 10.1016/j.jpcs.2019.109266

[2] N.N. Kuzmin, S.A. Klimin, B.N. Mavrin, K.N. Boldyrev, V.A. Chernyshev, B.V. Mill, M.N. Popova. Data in Brief, **28**, 104889 (2020). DOI: 10.1016/j.dib.2019.104889

[3] S.A. Klimin, A.B. Kuzmenko, M.N. Popova, B.Z. Malkin, I.V. Telegina. Phys. Rev. B, **82**, 174425-1 (2010). DOI: 10.1088/1742-6596/1389/1/012039

[4] A.D. Molchanova, K.N. Boldyrev, M.N. Popova, M.A. Prosnikov, R.M. Dubrovin, V.Yu. Davydov., R.V. Pisarev. Phys. Rev. B, **96**, 174305 (2017). DOI: 10.1103/PhysRevB.96.174305

[5] A.D. Molchanova, M.A. Prosnikov, V.P. Petrov, R.M. Dubrovin, S.G. Nefedov, D. Chernyshov, A.N. Smirnov, V.Yu. Davydov, K.N. Boldyrev, V.A. Chernyshev, R.V. Pisarev, M.N. Popova. J. All. Com., **865**, 158797 (2021). DOI: 10.1016/j.jallcom.2021.158797

[6] R.V. Pisarev, M.A. Prosnikov, V.Yu. Davydov, A.N. Smirnov, E.M. Roginskii, K.N. Boldyrev, A.D. Molchanova, M.N. Popova, M.B. Smirnov, V.Yu. Kazimirov. Phys. Rev. B, **93**, 134306 (2016). DOI: 10.1103/PhysRevB.93.134306

[7] M.A. Prosnikov, R.M. Dubrovin, A.D. Molchanova, K.N. Boldyrev, A.N. Smirnov, V.Yu. Davydov, A.M. Balbashov, M.N. Popova, R.V. Pisarev. Phys. of Solid State, **58** (12), 2427 (2016). DOI: 10.21883/ftt.2016.12.43868.239.

[8] K.N. Boldyrev, V.E. Anikeeva, O.I. Semenova, M.N. Popova. J. of Phys. Chem. C, **124** (42), 23307 (2020). DOI: 10.1021/acs.jpcc.0c06103

[9] D. Fausti, A. Nugroho, P. Loosdrecht, S.A. Klimin., M.N. Popova, L.N. Bezmaternykh. Phys. Rev. B, **74**, 024403 (2006). DOI: 10.1103/PhysRevB.74.024403

[10] S.A. Klimin, M.N. Popova, B.N. Mavrin, P.H.M. Loosdrecht, L.E. Svistov, A.I. Smirnov, L.A. Prozorova, H.-A. Krug von Nidda, Z. Seidov, A. Loidl, A.Ya. Shapiro, L.N. Demianets. Phys. Rev. B, **68**, 174408-1 (2003). DOI: 10.1103/PhysRevB.68.174408

[11] M.N. Popova, A.B. Sushkov, S.A. Klimin, E.P. Chukalina, B.Z. Malkin, M. Isobe, Yu. Ueda. Phys. Rev. B, **65**, 144303-1 (2002). DOI: 10.1103/PhysRevB.65.144303

[12] M.N. Popova, A.B. Sushkov, S.A. Golubchik, B.N. Mavrin, V.N. Denisov, B.Z. Malkin, A.I. Iskhakova, M. Isobe, Y. Ueda. JETP, **88**, 1186 (1999). DOI: 10.1134/1.558909.

[13] M.N. Popova, A.B. Sushkov, A.N. Vasil'ev, M. Isobe, Yu. Ueda. JETP Lett., **65**, 743 (1997). DOI: 10.1134/1.567420.

[14] S.A. Klimin, A.B. Kuzmenko, M.A. Kashchenko, M.N. Popova. Phys. Rev. B, **93**, 054304 (2016). DOI: 10.1103/PhysRevB.93.054304

[15] M.N. Popova, K.N. Boldyrev, S.A. Klimin, T.N. Stanislavchuk, A.A. Sirenko, L.N. Bezmaternykh. JMMM, **383**, 250 (2015). DOI: 10.1016/j.jmmm.2014.10.095.

[16] M.N. Popova. EPJ Web of Conferences, **132**, 01010 (2017). DOI: 10.1051/epjconf/201713201010

[17] M.N. Popova, K.N. Boldyrev. Phys. Usp., **62** (3), 275 (2019). DOI: 10.3367/UFNe.2018.06.038413.

[18] S.A. Klimin, E.A. Popova, M.N. Popova. J. of Physics: Conference Series, **1389**, 012039 (2019). DOI: 10.1088/1742-6596/1389/1/012039

[19] K.N. Boldyrev, T.N. Stanislavchuk, A.A. Sirenko, L.N. Bezmaternykh, M.N. Popova. Phys. Rev. B. Rapid Comm., **90**, 121101(R) (2014). DOI: 10.1103/PhysRevB.90.121101

[20] K.N. Boldyrev, B.N. Mavrin, M.N. Popova, L.N. Bezmaternykh. Opt. Spectrosc., **111** (3), 420 (2011). DOI: 10.1134/S0030400X11090049.

[21] R.V. Pisarev, K.N. Boldyrev, M.N. Popova, A.N. Smirnov, V.Yu. Davydov, L.N. Bezmaternykh, M.B. Smirnov, V.Yu. Kazimirov. Phys. Rev. B., **88**, 024301 (2013). DOI: 10.1103/PhysRevB.88.024301

[22] E.A. Vinogradov, V.A. Yakovlev, N.N. Novikova, M.N. Popova, S.K. Saikin, B.Z. Malkin. Solid State Comm., **142** (5), 256 (2007). DOI: 10.1016/j.ssc.2007.02.032

[23] P.S. Berdonosov, V.A. Dolgikh. J. Inorg. Chem., **53** (9), 1353 (2008). DOI: 10.1134/S0036023608090027.

[24] P.S. Berdonosov, E.S. Kuznetsova, V.A. Dolgikh. Crystals, **8** (4), 159 (2018). DOI: 10.3390/cryst8040159

[25] K.V. Zakharov, E.A. Zvereva, P.S. Berdonosov, E.S. Kuznetsova, V.A. Dolgikh, L. Clark, C. Black, P. Lightfoot, W. Kockelmann, Z.V. Pchelkina, S.V. Streltsov, O.S. Volkova, A.N. Vasiliev. Phys. Rev. B, **90** (21), 214417 (2014). DOI: 10.1103/PhysRevB.90.214417

[26] S.A. Klimin, P.S. Berdonosov, E.S. Kuznetsova, Fiz. Nizk. Temp. **47** (12), 1119 (2021). DOI: 10.1063/10.0007075

[27] K.V. Zakharov, E.A. Zvereva, E.S. Kuznetsova, P.S. Berdonosov, V.A. Dolgikh, M.M. Markina, A.V. Olenev, A.A. Shakin, O.S. Volkova, A.N. Vasiliev. J. Alloys Compounds, **685**, 442 (2016). DOI: 10.1016/j.jallcom.2016.05.213

[28] K.V. Zakharov, E.A. Zvereva, M.M. Markina, M.I. Stratan, E.S. Kuznetsova, S.F. Dunaev, P.S. Berdonosov, V.A. Dolgikh, A.V. Olenev, S.A. Klimin, L.S. Mazaev, M.A. Kashchenko, M.A. Ahmed, A. Banerjee, S. Bandyopadhyay, A. Iqbal, B. Rahaman, T. Saha-Dasgupta, A.N. Vasiliev. Phys. Rev. B, **94** (5), 054401 (2016). DOI: 10.1103/PhysRevB.94.054401

[29] M.M. Markina, K.V. Zakharov, E.A. Ovchenkov, P.S. Berdonosov, V.A. Dolgikh, E.S. Kuznetsova, A.V. Olenev, S.A. Klimin, M.A. Kashchenko, I.V. Budkin, I.V. Yatsyk, A.A. Demidov, E.A. Zvereva, A.N. Vasiliev. Phys. Rev. B, **96** (13), 134422 (2017). DOI: 10.1103/PhysRevB.96.134422

[30] S.A. Klimin, E.S. Kuznetsova, P.S. Berdonosov. Opt. Spectr., **130** (1), (2022), accepted

[31] S.A. Klimin, P.S. Berdonosov, E.S. Kuznetsova. Opt. Spectrosc., **129** (1), 47 (2021). DOI: 10.1134/S0030400X21010094.

[32] V. Gnezdilov, Yu. Pashkevich, P. Lemmens, V. Kurnosov, P. Berdonosov, V. Dolgikh, E. Kuznetsova, V. Pryadun, K. Zakharov, A. Vasiliev. Phys. Rev. B, **96** (11), 115144 (2017). DOI: 10.1103/PhysRevB.96.115144

[33] A. Pring, B.M. Gatehouse, W.D. Birch. Amer. Miner., **75** (11–12), 1421 (1990).

[34] P. Millet, B. Bastide, V. Pashchenko, S. Gnatchenko, V. Gapon, Y. Ksari, A. Stepanov. J. Mater. Chem., **11** (4), 1152 (2001). DOI: 10.1039/b007920k

[35] R. Becker, M. Johnsson. Solid State Sci., **7** (4), 375 (2005). DOI: 10.1016/j.solidstatesciences.2004.10.045

[36] R. Berrigan, B.M. Gatehouse. Acta Crystallogr. C: Struct. Sci. Comm., **52**, 496 (1996). DOI: 10.1107/S0108270195014120

[37] J.A. Mandarino. Eur. J. Miner., **6**, 337 (1994).
[38] S.V. Krivovichev, G.L. Starova, S.K. Filatov. Miner. Magazine, **63** (2), 263 (1999). DOI: 10.1180/minmag.1999.063.2.12
[39] E.V. Nazarchuk, S.V. Krivovichev, O.Y. Pankratova, S.K. Filatov. Phys. Chem. Miner., **27**, 440 (2000). DOI: 10.1007/s002699900079
[40] M. Pregelj, O. Zaharko, A. Gunther, A. Loidl, V. Tsurkan, S. Guerrero. Phys. Rev. B., **86** (14), 144409 (2012). DOI: 10.1103/PhysRevB.86.144409
[41] S.A. Nikolaev, V.V. Mazurenko, A.A. Tsirlin, V.G. Mazurenko. Phys. Rev. B., **94** (14), 144412 (2016). DOI: 10.1103/PhysRevB.94.144412
[42] I. Rousochatzakis, J. Richter, R. Zinke, A.A. Tsirlin. Phys. Rev. B., **91**, 024416 (2015). DOI: 10.1103/PhysRevB.91.024416
[43] M.M. Markina, P.S. Berdonosov, V.A. Dolgikh, K.V. Zakharov, E.S. Kuznetsova, A.N. Vasil'ev. Phys. Usp., **64**, 344 (2021). DOI: 10.3367/UFNe.2020.05.038773
[44] S.A. Klimin, M.S. Radionov, V.A. Yakovlev, N.N. Novikova, A.V. Peschanskii. Opt. Spectr., **129**, 42 (2021). DOI: 10.1134/S0030400X21010082
[45] R. Yankova, S. Genieva, N. Halachev, G. Dimitrova. J. Mol. Struct., **1106**, 82 (2016). DOI: 10.1016/j.molstruc.2015.10.091
[46] A. Bindu Gopinath, S. Devanarayanan. Indian J. Phys., **72B** (1), 75 (1998).
[47] Z. Mička, M. Daněk, J. Loub, B. Strauch, J. Podlanová, J. Hašek. J. Solid State Chem., **77** (2), 306 (1988). DOI: 10.1016/0022-4596(88)90253-8
[48] K.H. Miller, P.W. Stephens, C. Martin, E. Constable, R.A. Lewis, H. Berger, G.L. Carr, D.B. Tanner. Phys. Rev. B., **86**, 174104 (2012). DOI: 10.1103/PhysRevB.86.174104
[49] W. Theiß. Surf. Sci. Reports., **29** (3–4), 91 (1997). DOI: 10.1016/S0167-5729(96)00012-X
[50] G. Herzberg. *Molecular Spectra and Molecular Structure. Part II. Infrared and Raman Spectra of Polyatomic Molecules* (Van Nostrand Comp., New York, 1945)
[51] R.D. Shannon. Acta Crystallogr. A., **32**, 751 (1976). DOI: 10.1107/S0567739476001551
[52] Database of Ionic Radii [Electronic source]. URL: http://abulafia.mt.ic.ac.uk/shannon/ptable.php